

15. R. E. Slusher, L. W. Hollberg, B. Yurke, J. C. Mertz, J. F. Valley, *Phys. Rev. Lett.* **55**, 2409–2412 (1985).
16. L.-A. Wu, H. J. Kimble, J. L. Hall, H. Wu, *Phys. Rev. Lett.* **57**, 2520–2523 (1986).
17. D. T. Smithey, M. Beck, M. G. Raymer, A. Faridani, *Phys. Rev. Lett.* **70**, 1244–1247 (1993).
18. A. I. Lvovsky *et al.*, *Phys. Rev. Lett.* **87**, 050402 (2001).
19. N. B. Grosse, T. Symul, M. Stobinska, T. C. Ralph, P. K. Lam, *Phys. Rev. Lett.* **98**, 153603 (2007).
20. A. M. Fox, J. J. Baumberg, M. Dabbicco, B. Huttner, J. F. Ryan, *Phys. Rev. Lett.* **74**, 1728–1731 (1995).
21. M. E. Anderson, M. Beck, M. G. Raymer, J. D. Bierlein, *Opt. Lett.* **20**, 620–622 (1995).
22. C. Silberhorn *et al.*, *Phys. Rev. Lett.* **86**, 4267–4270 (2001).
23. P. J. Mosley *et al.*, *Phys. Rev. Lett.* **100**, 133601 (2008).
24. Q. Wu, X.-C. Zhang, *Appl. Phys. Lett.* **71**, 1285–1286 (1997).
25. A. Leitenstorfer, S. Hunsche, J. Shah, M. C. Nuss, W. H. Knox, *Appl. Phys. Lett.* **74**, 1516–1518 (1999).
26. K. Liu, J. Z. Xu, X.-C. Zhang, *Appl. Phys. Lett.* **85**, 863–865 (2004).
27. C. Kübler, R. Huber, S. Tübel, A. Leitenstorfer, *Appl. Phys. Lett.* **85**, 3360–3362 (2004).
28. S. Namba, *J. Opt. Soc. Am.* **51**, 76–79 (1961).
29. G. Gallot, D. Grischkowsky, *J. Opt. Soc. Am. B* **16**, 1204–1212 (1999).
30. A. S. Moskalenko, C. Riek, D. V. Seletskiy, G. Burkard, A. Leitenstorfer, <http://arxiv.org/abs/1508.06953> (2015).
31. R. Loudon, P. L. Knight, *J. Mod. Opt.* **34**, 709–759 (1987).
32. C. Fürst, A. Leitenstorfer, A. Laubereau, R. Zimmermann, *Phys. Rev. Lett.* **78**, 3733–3736 (1997).
33. A. A. Clerk, M. H. Devoret, S. M. Girvin, F. Marquardt, R. J. Schoelkopf, *Rev. Mod. Phys.* **82**, 1155–1208 (2010).

ACKNOWLEDGMENTS

Support by the European Research Council (Advanced Grant 290876 “UltraPhase”), by Deutsche Forschungsgemeinschaft (SFB767), and by NSF via a postdoctoral fellowship for D.V.S. (award no. 1160764) is gratefully acknowledged.

SUPPLEMENTARY MATERIALS

www.sciencemag.org/content/350/6259/420/suppl/DC1
Materials and Methods
Figs. S1 to S5
References (34–40)

8 July 2015; accepted 16 September 2015
Published online 1 October 2015
10.1126/science.aac9788

ASTEROSEISMOLOGY

Asteroseismology can reveal strong internal magnetic fields in red giant stars

Jim Fuller,^{1,2,*†} Matteo Cantiello,^{2,*†} Dennis Stello,^{3,4} Rafael A. Garcia,⁵ Lars Bildsten^{2,6}

Internal stellar magnetic fields are inaccessible to direct observations, and little is known about their amplitude, geometry, and evolution. We demonstrate that strong magnetic fields in the cores of red giant stars can be identified with asteroseismology. The fields can manifest themselves via depressed dipole stellar oscillation modes, arising from a magnetic greenhouse effect that scatters and traps oscillation-mode energy within the core of the star. The Kepler satellite has observed a few dozen red giants with depressed dipole modes, which we interpret as stars with strongly magnetized cores. We find that field strengths larger than $\sim 10^5$ gauss may produce the observed depression, and in one case we infer a minimum core field strength of $\approx 10^7$ gauss.

Despite rapid progress in the discovery and characterization of magnetic fields at the surfaces of stars, very little is known about internal stellar magnetic fields. This has prevented the development of a coherent picture of stellar magnetism and the evolution of magnetic fields within stellar interiors.

After exhausting hydrogen in their cores, most main sequence stars evolve up the red giant branch (RGB). During this phase, the stellar structure is characterized by an expanding convective envelope and a contracting radiative core. Acoustic waves (p modes) in the envelope can

couple to gravity waves (g modes) in the core (1). Consequently, nonradial stellar oscillation modes become mixed modes that probe both the envelope (the p-mode cavity) and the core (the g-mode cavity), as illustrated in Fig. 1. Mixed modes (2) have made it possible to distinguish between hydrogen- and helium-burning red giants (3, 4) and have been used to measure the rotation rate of red giant cores (5, 6).

A group of red giants with depressed dipole modes were identified using observations from the Kepler satellite [(7), see also Fig. 2]. These stars show normal radial modes (spherical harmonic degree $\ell = 0$) but exhibit dipole ($\ell = 1$) modes whose amplitude is much lower than usual. Until now, the suppression mechanism was unknown (8). Below, we demonstrate that dipole mode suppression may result from strong magnetic fields within the cores of these red giants.

Red giant oscillation modes are standing waves that are driven by stochastic energy input from turbulent near-surface convection (9, 10). Waves excited near the stellar surface propagate downward as acoustic waves until their angular frequency ω is less than the local Lamb frequency for waves of angular degree ℓ ; i.e., until $\omega = L_\ell = \sqrt{\ell(\ell+1)}v_s/r$, where v_s is the local sound speed and r is the radial coordinate. At this bound-

dary, part of the wave flux is reflected, and part of it tunnels into the core.

The wave resumes propagating inward as a gravity wave in the radiative core where $\omega < N$, where N is the local buoyancy frequency. In normal red giants, wave energy that tunnels into the core eventually tunnels back out to produce the observed oscillation modes. We show here that suppressed modes can be explained if wave energy leaking into the core never returns back to the stellar envelope.

The degree of wave transmission between the core and envelope is determined by the tunneling integral through the intervening evanescent zone. The transmission coefficient is

$$T \sim \left(\frac{r_1}{r_2}\right)^{\sqrt{\ell(\ell+1)}} \quad (1)$$

where r_1 and r_2 are the lower and upper boundaries of the evanescent zone, respectively. The fraction of wave energy transmitted through the evanescent zone is T^2 . For waves of the same frequency, larger values of ℓ have larger values of r_2 , thus Eq. 1 demonstrates that high ℓ waves have much smaller transmission coefficients through the evanescent zone.

The visibility of stellar oscillations depends on the interplay between driving and damping of the modes (10, 11). To estimate the reduced mode visibility due to energy loss in the core, we assume that all mode energy that leaks into the g-mode cavity is completely lost. The mode then loses a fraction T^2 of its energy in a time $2t_{\text{cross}}$, where t_{cross} is the wave crossing time of the acoustic cavity. Due to the larger energy loss rate, the mode has less energy E_{ac} within the acoustic cavity and produces a smaller luminosity fluctuation V at the stellar surface, whose amplitude scales as $V^2 E_{\text{ac}}$. We show (12) that the ratio of visibility between a suppressed mode V_{sup} and its normal counterpart V_{norm} is

$$\frac{V_{\text{sup}}^2}{V_{\text{norm}}^2} = [1 + \Delta\nu \tau T^2]^{-1} \quad (2)$$

where $\Delta\nu \approx (2t_{\text{cross}})^{-1}$ (13) is the large frequency separation between acoustic overtone modes, and τ is the damping time of a radial mode with similar frequency. We evaluate T^2 from our stellar models using Eq. 6, whereas $\tau \approx 5$ to 10 days (10, 14–16) for stars ascending the RGB.

¹TAPIR, Walter Burke Institute for Theoretical Physics, Mailcode 350-17 California Institute of Technology, Pasadena, CA 91125, USA. ²Kavli Institute for Theoretical Physics, University of California, Santa Barbara, CA 93106, USA. ³Sydney Institute for Astronomy, School of Physics, University of Sydney, New South Wales 2006, Australia. ⁴Stellar Astrophysics Centre, Department of Physics and Astronomy, Aarhus University, Ny Munkegade 120, DK-8000 Aarhus C, Denmark. ⁵Laboratoire Astrophysique Interactions Multi-échelles, Commissariat à l'Énergie Atomique/Direction des Sciences de la Matière, CNRS, Université Paris Diderot, Institut de Recherches sur les lois Fondamentales de l'Univers/Service d'Astrophysique Centre de Saclay, 91191 Gif-sur-Yvette Cedex, France. ⁶Department of Physics, University of California, Santa Barbara, CA 93106, USA.

*Corresponding author. E-mail: jfuller@caltech.edu (J.F.); matteo@kitp.ucsb.edu (M.C.) †These authors contributed equally to this work.

Most observed modes are near the frequency ν_{\max} , which is determined by the evolutionary state of the star. On the RGB, more-evolved stars generally have smaller ν_{\max} . Figure 2 compares our estimate for suppressed dipole mode visibility (Eq. 2) with Kepler observations (7, 8). The objects identified by (7) as depressed dipole mode stars lie very close to our estimate. The striking agreement holds over a large baseline in ν_{\max} extending from the very early red giants KIC8561221 (8) and KIC9073950 at high ν_{\max} to near the luminosity bump at low ν_{\max} . The observations are consistent with nearly total wave energy loss in the core, because partial energy loss would create stars with less-depressed modes, which seem to be rare.

We conclude that the cores of stars with depressed dipole modes efficiently trap or disrupt waves tunneling through the evanescent region. This is further supported by their normal $\ell = 0$ mode visibility, because radial modes do not propagate within the inner core, and because much larger field strengths are required to alter acoustic waves. The absence (or perhaps smaller degree) of depression observed for $\ell = 2$ modes (7) occurs because quadrupole modes have a smaller transmission coefficient T , and less of their energy leaks into the core.

An additional consequence is that the larger effective damping rate for depressed modes will lead to larger linewidths in the oscillation power spectrum. The linewidth of a depressed dipole mode is $\tau^{-1} + \Delta\nu T_{\ell}^2$ and is generally much larger than that of a normal mode. The depressed dipole modes in KIC8561221 (8) indeed have much larger linewidths than normal dipole modes in similar stars.

Magnetic fields can provide the mechanism for trapping oscillation mode energy in the core by altering gravity wave propagation. The nearly horizontal motions and short radial wavelengths of gravity waves in RGB cores will bend radial magnetic field lines, creating strong magnetic tension forces. The acceleration required to restore a wave of angular frequency ω and horizontal displacement ξ_h is $\xi_h \omega^2$, whereas the magnetic tension acceleration due to a radial magnetic field of strength B_r is $\xi_h B_r^2 k_r^2 / (4\pi\rho)$, where k_r is the radial wavenumber and ρ is the density. Gravity waves are strongly altered by the magnetic fields when the magnetic tension force dominates, which for dipole waves occurs at a critical magnetic field strength (12)

$$B_c = \sqrt{\frac{\pi\rho}{2}} \frac{\omega^2 r}{N} \quad (3)$$

This field strength approximately corresponds to the point at which the Alfvén speed becomes larger than the radial group velocity of gravity waves.

Magneto-gravity waves cannot exist in regions with $B_r > B_c$, where magnetic tension overwhelms the buoyancy force; i.e., the stiff field lines cannot be bent by the placid gravity wave motion. Consequently, dipole magneto-gravity waves become evanescent when $\omega < \omega_{MG}$,

where the magneto-gravity frequency ω_{MG} is defined as

$$\omega_{MG} = \left[\frac{2 B_r^2 N^2}{\pi \rho r^2} \right]^{1/4} \quad (4)$$

Figure 3 shows a wave propagation diagram in which a strong internal magnetic field prevents magneto-gravity wave propagation in the core.

In red giants, B_c is typically smallest at the peak in N corresponding to the sharp density gradient within the hydrogen-burning (H-burning) shell. Therefore, gravity waves are most susceptible to magnetic alteration in the H-burning shell, and the observation of a star with depressed dipole modes thus provides a lower limit to the radial field strength (Eq. 3) evaluated in the H-burning shell. We refer to this field strength as $B_{c,\min}$. Magnetic

Fig. 1. Wave propagation in red giants with magnetized cores.

Acoustic waves excited in the envelope couple to gravity waves in the radiative core. In the presence of a magnetic field in the core, the gravity waves are scattered at regions of high field strength. Because the field cannot be spherically symmetric, the waves are scattered to high angular degree ℓ and become trapped within the core, where they eventually dissipate (dashed wave with arrow). We refer to this as the magnetic greenhouse effect.

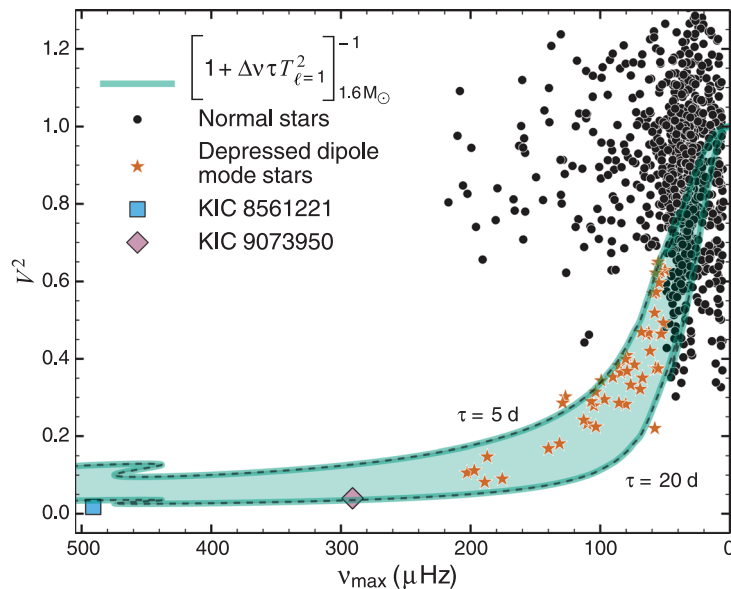
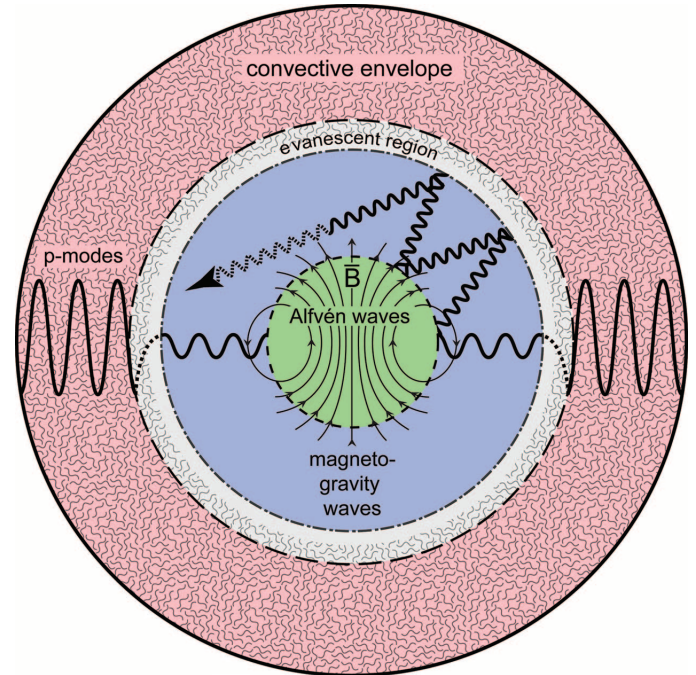


Fig. 2. Normalized visibility of dipolar modes as a function of ν_{\max} . The star and circle symbols represent the observed visibility V^2 of $\ell = 1$ modes (12). The data are taken from (7) and divided by 1.54, so that in normal oscillators, the average visibility is $V^2 = 1$ (22). Stars with depressed dipole modes (orange stars) are identified following the same criteria as in (7). The theoretical band shows the visibility of depressed dipole modes in a $1.6 M_{\odot}$, where M_{\odot} is the mass of the sun, star, as predicted by Eq. 2, and is quite insensitive to the mass of the model. The visibility of the depressed dipoles in KIC 8561221 (8) and KIC 9073950 is also shown (square and diamond symbols, respectively). We used values for τ in the range of 5 to 20 days, consistent with (10, 16).

Fig. 3. Propagation diagram for a magnetized red giant model.

The model has $M = 1.6 M_{\odot}$, $R = 6.6 R_{\odot}$, $v_{\max} = 120 \mu\text{Hz}$, and a core magnetic field of $\approx 6 \times 10^6 \text{ G}$ (fig. S1).

(A) The red, blue, and green lines are the dipole Lamb frequency L_1 , the buoyancy frequency N , and the magneto-gravity frequency ω_{MG} (defined in Eq. 4), respectively. Regions are colored by the types of waves they support: The red region is the acoustic wave cavity, the blue region is the magneto-gravity wave cavity, and the green region hosts only Alfvén waves. The horizontal line is the frequency of maximum power, v_{\max} , for this stellar model. Waves at this frequency behave like

acoustic waves near the surface, magneto-gravity waves in the outer core, and Alfvén waves in the inner core. (B) Critical radial magnetic field strength B_c needed to suppress dipole modes. B_c (Eq. 3) is evaluated at the angular frequency $\omega = 2\pi v_{\max}$. B_c has a sharp minimum at the H-burning shell, which determines the minimum field strength $B_{c,\min}$ required for dipole mode suppression.

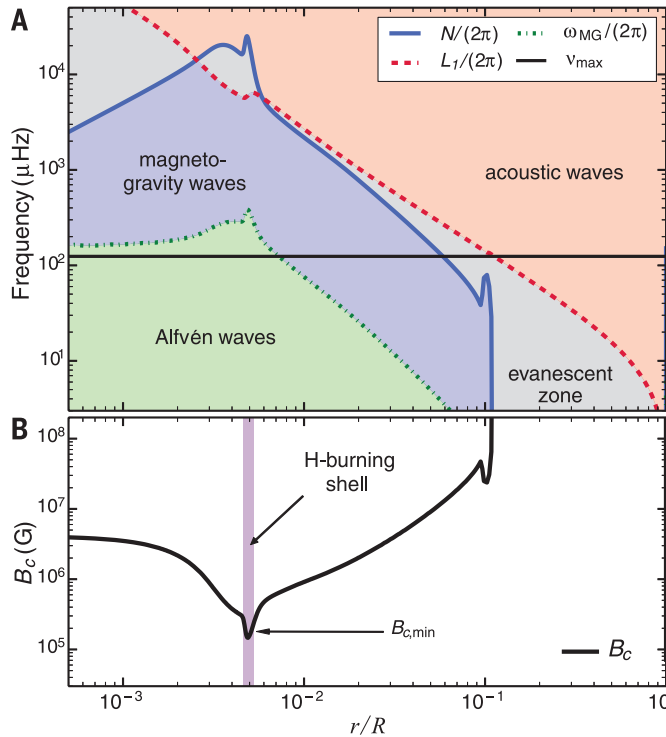
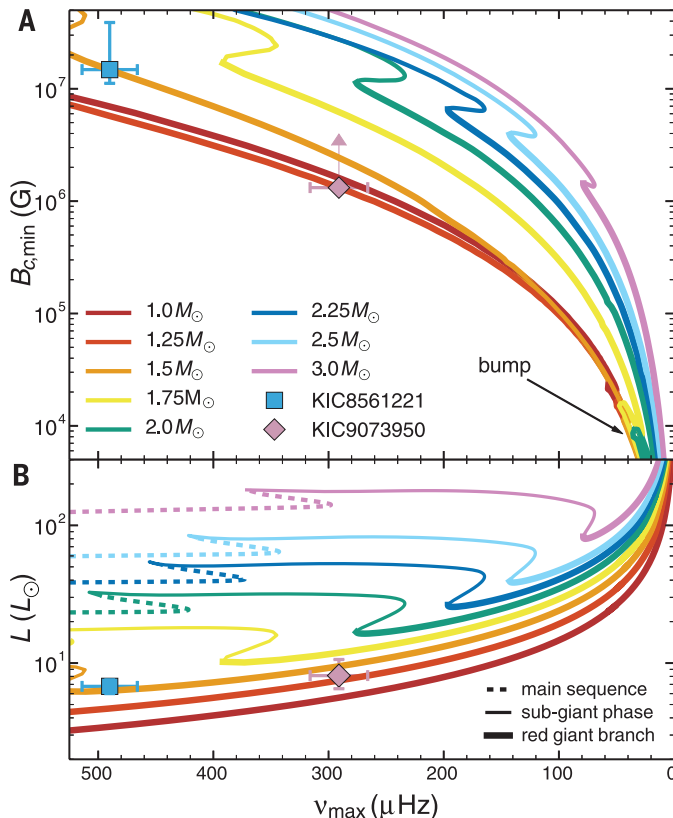


Fig. 4. Minimum field strength $B_{c,\min}$ required for magnetic suppression of dipole oscillation modes in stars evolving up the RGB.

(A) $B_{c,\min}$ is shown as a function of the frequency of maximum power, v_{\max} , for stars of different mass. L , luminosity; L_{\odot} , luminosity of the Sun. $B_{c,\min}$ has been computed for modes with angular frequency $\omega = 2\pi v_{\max}$. We have labeled the observed value of v_{\max} and inferred core field strength B_r for the lower RGB star KIC8561221 (8) and a lower limit to the field strength in KIC9073950. (B) Asteroseismic HR diagram showing stellar evolution tracks over the same range in v_{\max} . Stars evolve from left to right as they ascend the RGB. Dashed lines show the end of main sequence evolution, thin solid lines are the sub-giant phase, and thick solid lines are the RGB. We do not show any evolution beyond the RGB (i.e., no clump or asymptotic giant branch).



suppression via horizontal fields can also occur, but in general requires much larger field strengths.

In stars with field strengths exceeding B_c (Eq. 3) somewhere in their core, incoming dipole gravity waves will become evanescent where $B_r > B_c$. At this point, the waves must either reflect or be transmitted into the strongly magnetized region as Alfvén waves. In either case, the reflection/transmission process modifies the angular structure of the waves so that their energy is spread over a broad spectrum of ℓ values (12). Once a dipole wave has its energy transferred to higher values of ℓ , it will not substantially contribute to observable oscillations at the stellar surface, because higher- ℓ waves are trapped within the radiative core by a thicker evanescent region (Eq. 1 and Fig. 1) separating the core from the envelope. Even if some wave energy does eventually return to the surface to create an oscillation mode, the increased time spent in the core results in a very large mode inertia, greatly reducing the mode visibility. Additionally, high- ℓ waves will not be detected in Kepler data because of the geometric cancellation, which makes $\ell > 3$ modes nearly invisible (17).

The magnetic greenhouse effect arises not from the alteration of incoming wave frequencies but rather from modification of the wave angular structure. Such angular modification originates from the inherently nonspherical structure of even the simplest magnetic field configurations.

Dipole oscillation modes can be suppressed if the magnetic field strength exceeds B_c (Eq. 3) at some point within the core. We therefore posit that stars with depressed dipole oscillation modes have minimum core field strengths of $B_{c,\min}$. Stars with normal dipole oscillation modes cannot have radial field strengths in excess of $B_{c,\min}$ within their H-burning shells. However, they may contain larger fields away from the H-burning shell, or they may contain fields that are primarily horizontal (e.g., strong toroidal fields).

Figure 4 shows the value of $B_{c,\min}$ as stars evolve up the RGB. We have calculated $B_{c,\min}$ for angular frequencies $\omega = 2\pi v_{\max}$ and evaluated v_{\max} using the scaling relation proposed by (18). On the lower RGB, where $v_{\max} \geq 250 \mu\text{Hz}$, field strengths on the order of $B_{c,\min} \geq 10^6 \text{ G}$ are required for magnetic suppression. As stars evolve up the RGB, the value of $B_{c,\min}$ decreases sharply, primarily because v_{\max} decreases. By the luminosity bump (near $v_{\max} \sim 40 \mu\text{Hz}$), field strengths of only $B_{c,\min} \sim 10^4 \text{ G}$ are sufficient for magnetic suppression. Magnetic suppression during the sub-giant phase (higher v_{\max}) and in higher-mass stars ($M \geq 2 M_{\odot}$) may be less common due to the larger field strengths required.

For a given field strength, there is a transition frequency v_c below which modes will be strongly suppressed and above which modes will appear normal. Stars that show this transition are especially useful because they allow for an inference of B_r at the H-burning shell via Eq. 3, evaluated at the transition frequency $\omega = 2\pi v_c$. The RGB star KIC8561221 shows this transition (8). Using the observed value of $v_c \approx 600 \mu\text{Hz}$, we infer that the radial component of the magnetic field

within the H-burning shell is $B_r \approx 1.5 \times 10^7$ G, although we cannot rule out the presence of stronger fields away from the H-burning shell. This large field strength may indicate that KIC8561221 is the descendant of a magnetic A-type star whose internal field was much stronger than the typical surface fields of $B \sim 3$ kG of A-type stars (19).

In principle, it is possible that another symmetry-breaking mechanism within the core could suppress dipole mode amplitudes. The only other plausible candidate is rapid core rotation. In order for rotation to strongly modify the incoming waves so that they will be trapped in the core, the core must rotate at a frequency comparable to v_{\max} , roughly two orders of magnitude faster than the values commonly measured in red giant cores (2, 6, 20). The depressed dipole mode star KIC8561221 (8) does not exhibit rapid core rotation and disfavors the rotation scenario.

A magnetic field of amplitude $B > 10^4$ G (Fig. 4) could be present in the core of a red giant if it was retained from previous phases of stellar formation and evolution (12). These strong fields may reside within the inner core with little external manifestation apart from the reduced visibility of the dipole modes. However, fields of similar amplitude have been discussed in order to explain the suppression of thermohaline mixing in a small fraction of red giant stars, as inferred from the observations of their surface abundances (21). The inferred core field strength of $B_r \geq 1.5 \times 10^7$ G in KIC8561221 shows that very strong magnetic fields ($B \gg 10^6$ G) can exist within the radiative cores of early RGB stars. Because these fields are probably inherited from previous stages of stellar evolution, slightly weaker ($B \gg 10^5$ G) fields could exist in the cores of exceptional very highly magnetized main sequence stars.

REFERENCES AND NOTES

1. T. R. Bedding, *Solar-like Oscillations: An Observational Perspective* (Cambridge Univ. Press, Cambridge, 2014).
2. P. G. Beck et al., *Science* **332**, 205 (2011).
3. T. R. Bedding et al., *Nature* **471**, 608–611 (2011).
4. B. Mosser et al., *Astron. Astrophys.* **572**, L5 (2014).
5. P. G. Beck et al., *Nature* **481**, 55–57 (2011).
6. B. Mosser et al., *Astron. Astrophys.* **548**, A10 (2012).
7. B. Mosser et al., *Astron. Astrophys.* **537**, A30 (2012).
8. R. A. García et al., *Astron. Astrophys.* **563**, A84 (2014).
9. P. Goldreich, D. A. Keeley, *Astrophys. J.* **212**, 243 (1977).
10. M.-A. Dupret et al., *Astron. Astrophys.* **506**, 57–67 (2009).
11. O. Benomar et al., *Astrophys. J.* **781**, L29 (2014).
12. See the supplementary materials on Science Online.
13. W. J. Chaplin, A. Miglio, *Annu. Rev. Astron. Astrophys.* **51**, 353–392 (2013).
14. E. Corsaro et al., *Astrophys. J.* **757**, 190 (2012).
15. M. Grosjean et al., *Astron. Astrophys.* **572**, A11 (2014).
16. E. Corsaro, J. De Ridder, R. A. García, *Astron. Astrophys.* **579**, A83 (2015).
17. T. R. Bedding et al., *Astrophys. J.* **713**, L176–L181 (2010).
18. T. M. Brown, R. L. Gilliland, R. W. Noyes, L. W. Ramsey, *Astrophys. J.* **368**, 599 (1991).
19. M. Aurière et al., *Astron. Astrophys.* **475**, 1053–1065 (2007).
20. S. Deheuvels et al., *Astron. Astrophys.* **564**, A27 (2014).
21. C. Charbonnel, J.-P. Zahn, *Astron. Astrophys.* **476**, L29–L32 (2007).
22. J. Ballot, C. Barban, C. V. Veer-Menneret, *Astron. Astrophys.* **531**, A124 (2011).

ACKNOWLEDGMENTS

The authors of this paper thank the Kavli Institute for Theoretical Physics and the organizers of the Galactic Archaeology and Precision Stellar Astrophysics program held from January to April 2015. J.F. acknowledges partial support from NSF under grant no. AST-1205732 and through a Lee DuBridge Fellowship at the California Institute of Technology. R.A.G. acknowledges the support of the European Community's Seventh Framework Programme (FP7/2007-2013) under grant agreement no. 312844 (SPACEINN), and from the Centre National d'Études Spatiales. D.S. acknowledges support from the Australian Research Council. This project was supported by NASA under Theory and

Computational Astrophysics Network grant no. NNX14AB53G and NSF under grants PHY 11-25915 and AST 11-09174.

SUPPLEMENTARY MATERIALS

www.sciencemag.org/content/350/6259/423/suppl/DC1
Supplementary Text
Figs. S1 to S3
Table S1
References (23–56)

29 May 2015; accepted 15 September 2015
10.1126/science.aac6933

PLANT DEVELOPMENT

Transcriptional control of tissue formation throughout root development

Miguel A. Moreno-Risueno,¹ Rosangela Sozzani,^{2*} Galip Gürkan Yardımcı,^{2†} Jalean J. Petricka,^{2‡} Teva Vernoux,³ Ikram Bililou,⁴ Jose Alonso,⁵ Cara M. Winter,² Uwe Ohler,⁶ Ben Scheres,⁴ Philip N. Benfey^{2§}

Tissue patterns are dynamically maintained. Continuous formation of plant tissues during postembryonic growth requires asymmetric divisions and the specification of cell lineages. We show that the BIRDS and SCARECROW regulate lineage identity, positional signals, patterning, and formative divisions throughout *Arabidopsis* root growth. These transcription factors are postembryonic determinants of the ground tissue stem cells and their lineage. Upon further activation by the positional signal SHORT-ROOT (a mobile transcription factor), they direct asymmetric cell divisions and patterning of cell types. The BIRDS and SCARECROW with SHORT-ROOT organize tissue patterns at all formative steps during growth, ensuring developmental plasticity.

Organs are formed, patterned, and maintained during growth. In the root of *Arabidopsis*, tissues are organized as concentric cylinders around the internal vascular tissue. Much progress has been made in identifying factors responsible for patterning some of these tissues, such as the ground tissue. The ground tissue lineage is continuously generated by the cortex endodermis initial stem cell (CEI), which divides in the transverse orientation (anticlinal division) to produce a daughter cell (CEID) and regenerate itself. The ground tissue is patterned when the CEID divides asymmetrically in the longitudinal (periclinal) orientation, gen-

erating two cell types: endodermis and cortex (1). The mobile transcription factor SHORT-ROOT (SHR) moves from the stele to the ground tissue, where SCARECROW (SCR) and the C_2H_2 transcription factor JACKDAW (JKD) sequester it in the nucleus. Nuclear SHR is required for the periclinal asymmetric divisions of the CEID that pattern the ground tissue (2, 3). These divisions are activated through a bistable switch involving SHR, SCR, and other components and correlate with the temporal activation of transcriptional programs (4, 5). Absence of SHR results in abnormal ground tissue patterning, with loss of the endodermis and a remaining single layer of ground tissue due to absence of asymmetric cell divisions (5, 6). Because the ground tissue lineage remains, this indicates that other factors participate in its specification.

Specific roles for JKD and several close relatives have been recently identified (7). JKD and BALD-IBIS regulate SHR movement by promoting its nuclear retention, and cooperatively with MAGPIE (MGP) and NUTCRACKER (NUC) are required for the formative divisions that pattern the ground tissue into cortex and endodermis. Here we show that JKD, MGP, and NUC, along with two new members of this family (collectively known as the BIRDS; table S1) named BLUEJAY (BLJ) and IMPERIAL EAGLE (IME), organize the ground tissue after embryogenesis. They function

¹Department of Biotechnology, Center for Plant Genomics and Biotechnology, Universidad Politécnica de Madrid, 28223 Pozuelo de Alarcón (Madrid), Spain. ²Department of Biology and Howard Hughes Medical Institute, Duke University, Durham, NC 27708, USA. ³Laboratoire de Reproduction et Développement des Plantes, CNRS, INRA, ENS Lyon, UCBL, Université de Lyon, 69364 Lyon, France. ⁴Department of Plant Biology, Wageningen University Research, Wageningen, Netherlands. ⁵Department of Plant and Microbial Biology, North Carolina State University, Raleigh, NC 27695, USA. ⁶Berlin Institute for Medical Systems Biology, Max Delbrück Center for Molecular Medicine, 13125 Berlin, Germany. *Present address: Department of Plant and Microbial Biology, North Carolina State University, Raleigh, NC 27695, USA. †Present address: Department of Genome Sciences, University of Washington, Seattle, WA 98195, USA. ‡Present address: Carleton College, Northfield, MN 55057, USA. §Corresponding author. E-mail: philip.benfey@duke.edu



Asteroseismology can reveal strong internal magnetic fields in red giant stars

Jim Fuller *et al.*

Science **350**, 423 (2015);

DOI: 10.1126/science.aac6933

This copy is for your personal, non-commercial use only.

If you wish to distribute this article to others, you can order high-quality copies for your colleagues, clients, or customers by [clicking here](#).

Permission to republish or repurpose articles or portions of articles can be obtained by following the guidelines [here](#).

The following resources related to this article are available online at www.sciencemag.org (this information is current as of October 22, 2015):

Updated information and services, including high-resolution figures, can be found in the online version of this article at:

<http://www.sciencemag.org/content/350/6259/423.full.html>

Supporting Online Material can be found at:

<http://www.sciencemag.org/content/suppl/2015/10/21/350.6259.423.DC1.html>

This article **cites 52 articles**, 8 of which can be accessed free:

<http://www.sciencemag.org/content/350/6259/423.full.html#ref-list-1>

This article appears in the following **subject collections**:

Astronomy

<http://www.sciencemag.org/cgi/collection/astronomy>